Sensitivity Analysis of External-Rotor Permanent Magnet Assisted Synchronous Reluctance Motor

Hadi Aghazadeh, Seyed Ebrahim Afjei, Alireza Siadatan

Abstract—In this paper, a proper approach is taken to assess a set of the most effective rotor design parameters for an external-rotor permanent magnet assisted synchronous reluctance motor (PMaSynRM) and therefore to tackle the design complexity of the rotor structure. There are different advantages for introducing permanent magnets into the rotor flux barriers, some of which are to saturate the rotor iron ribs, to increase the motor torque density and to improve the power factor. Moreover, the d-axis and q-axis inductances are of great importance to simultaneously achieve maximum developed torque and low torque ripple. Therefore, sensitivity analysis of the rotor geometry of an 8-pole external-rotor permanent magnet assisted synchronous reluctance motor is performed. Several magnetically accurate finite element analyses (FEA) are conducted to characterize the electromagnetic performance of the motor. The analyses validate torque and power factor equations for the proposed external-rotor motor. Based upon the obtained results and due to an additional term, permanent magnet torque, added to the reluctance torque, the electromagnetic torque of the PMaSynRM increases.

Keywords—Permanent magnet assisted synchronous reluctance motor, flux barrier, flux carrier, electromagnetic torque, and power factor.

I. INTRODUCTION

COMPARED to classical induction machines, synchronous reluctance machine (SynRM) has limited applications due to its features such as poor efficiency, low power factor and high torque ripple for many years. But, because of recent developments in the modern power electronic converters and electric drive systems, SynRM and particularly permanent magnet assisted synchronous reluctance motor (PMaSynRM) are considered as the main competitors to permanent magnet (PM) motors. The unique value of PMaSynRM in combining the advantages of SyRM and PM machine ends in a high efficient as well as cost effective machines. The design of SynRM motor has been a challenging subject of research since the introduction of this machine in 1923 [1]. These investigations can be mainly divided into two classes: first, maximizing motor torque density and second, minimizing motor torque ripple and consequently increasing produced torque quality.

A tremendous amount of efforts have been given to developing the in-wheel type electric motors with high torque density and low torque ripple for traction applications [2].

Hadi Aghazadeh is with the Department of Electrical and Computer Engineering, Shahid Beheshti University, Tehran, Iran (e-mail: H_aghazadeh@sbu.ac.ir).
Seyed Ebrahim Afjei and Alireza Siadatan are with the Department of Electrical and Computer Engineering, Shahid Beheshti University, Tehran, Iran.

External rotor topology is more practically suitable for some applications such as wind turbine, fan, and compressors where the outside of the machine rotates [3], [5]. The external rotor motor provides several unique values over inner rotor motor, some of which are larger rotor diameter, wider stator slot area which in turn increase torque density and provide better performance characteristics [6]. External rotor induction motor with larger inertia provides wide constant speed operation area for varying load conditions [4]. Furthermore, in the external rotor architecture, the torque density can be further enhanced using high motor pole number. By contrast, for internal-rotor topology, the idea of increasing the ratio of d-axis and q-axis inductance, saliency ratio, and having high pole number are conflicting and therefore pole numbers up to 8 are rarely found in the literatures. For the first time, an outer rotor synchronous reluctance motor with low power was proposed for propulsion of an electric bike in [7]. A 1.2 kW 5-pole paired with 48-slot stator External rotor ferrite based synchronous reluctance motor has been suggested for electric two-wheeler application in [8]. Multi-phase external rotor PMaSynRM has been presented for its advantages such as high power density, low back-EMF harmonics content and low torque ripple in [9], [10]. The feasibility study of developing an external-rotor synchronous reluctance motor and the effect of rotor geometry on the output-Torque in a direct drive application in comparison with Switched reluctance motor are studied in [11].

Generally, three different rotor structures are used in SynRM: simple salient, axially laminated anisotropy (ALA) and transversally laminated anisotropy (TLA). Saliency ratio higher than 10 mostly can be achieved by ALA structure, whereas the TLA rotor presents amounts less than 5. However, TLA is preferred seeing as manufacturing procedure by simply punching and stacking of the rotor laminations. The SynRM rotor has a complex and anisotropic structure and lots of geometrical factors are involved in the rotor's flux barriers and carriers dimensioning. Some of the previous efforts to tackle the complexity of this problem can be found in [12], [13]. Most of the literatures use an analytical method which is based on a lumped equivalent magnetic model of the machine without or with considering the saturation effect, but these methods are not accurate enough because FEM tool has to be used partly to modify the optimization result.

In this paper, an approach is taken to assess a set of most effective rotor design parameters, which have to be considered for an external-rotor PMaSynRM. FEM parameter sensitivity analysis method is used for PMaSynRM to investigate the influence of geometrical parameters on machine magnetic performance in order to achieve optimized rotor geometry.

World Academy of Science, Engineering and Technology
International Journal of Energy and Power Engineering
Vol:12, No:6, 2018

Furthermore, performance evaluation of PMaSynRM in comparison with SynRM is finally reported.

II. STRUCTURE AND PRINCIPLE OF THE EXTERNAL-ROTOR PMASYNRM

The SynRM rotor has a complex and anisotropic structure and lots of geometrical parameters are involved in the rotor's flux barriers and carriers dimensioning. In a PMaSynRM flux barriers are employed not only to shape the anisotropy structure of the rotor but also to place the PM. The iron paths in the rotor are the magnetic paths defined by the barriers and are referred as flux carriers. The geometry of an external-rotor and related parameters definition for SynRM with three interior barriers is shown in Fig. 1.

In FEA of the motor, it is extremely important to define the geometric parameters of the rotor which play the key role in the performance of the machine. The d-axis and q-axis inductances are of great importance in the electromagnetic performance of the synchronous reluctance motor. The rotor geometry should maximize the magnetic flux in direct axis meanwhile should minimize the flux in the quadratic axis. Hence, in order to maximize the flux in the d-axis and accordingly d-axis inductance, the flux carriers should be wide enough, whereas the increase in the width of barrier increases the q-axis inductance.
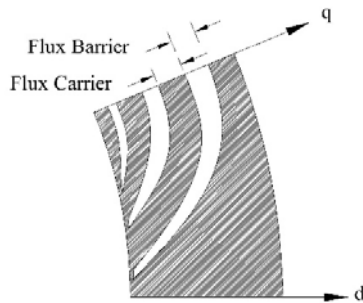

Fig. 1 External-rotor geometry and its related parameters definition for SynRM with three interior barriers

A. Electromagnetic Torque and Power Factor Calculation

The electromagnetic torque of the PMaSynRM can be simply obtained by:

$$T_{em} = \frac{3}{2} p \left(\lambda_d i_{qm} - \lambda_q i_{dm} \right) \tag{1}$$

$$\lambda_d = L_d (i_{dm}) i_{dm}$$

$$\lambda_q = L_q i_{qm} - \lambda_{pm}$$

$$T_{em} = \frac{3}{2} p \left(\lambda_{pm} i_{dm} + \left(L_d - L_q \right) i_{qm} i_{dm} \right)$$

where p is the number of pole pair, λ_{pm} is the PM flux linkage, L_d and L_q are the magnetizing inductances, i_{dm} and i_{qm} are the magnetizing currents, in d-axis and q-axis, respectively. Eelectromagnetic torque is produced by the magnets and the anisotropy of the rotor which is represented by the difference

between the inductance in the d-axis and q- axis (L_d - L_q). Thus, the resultant torque can be increased either if PM increases, or if the anisotropy of the rotor is increased, by increasing the difference between the inductances in d-axis and q-axis. It is worth mentioning that adding the PM in the q-axis creates flux linkage which compensates the flux $L_q i_{qm}$ and as a consequence decreases the q-axis flux. Moreover, the flux created by the PM saturates the iron ribs which reduce the inductance in the q-axis.

Additionally, to maximize the power factor, the ratio of these inductances (ξ) should be as high as possible. The maximum internal power factor is also presented as follows:

$$PF\bigg|_{max} = \cos\left(\varphi_i\right)\bigg|_{max} = \frac{\xi - 1}{\xi + 1} \tag{2}$$

$$\xi = \frac{L_{dm}\left(i_{dm}\right)}{L_{qm}}$$

B. General Rule for the Rotor Design

Stator produced magneto-motive force (MMF) in synchronous reference frame has two components from the rotor point of view in the d-axis (where the rotor has minimum reluctance) and the q-axis (where the rotor has maximum reluctance), which are MMF_d and MMF_q, respectively.

Normally, the rotor structure must satisfy the following requirements [14]:
- The direct-axis flux has to flow across the whole pole surface in order to obtain a large magnetizing inductance, L_d.
- The quadrate-axis flux needs to be minimized in order to get a low L_q.

Therefore, the iron segments in the rotor body which carries the magnetic flux should be in accordance with the natural flux line shape. The flux line distribution of an external 8 pole motor with three flux-barriers is depicted in Fig. 2.
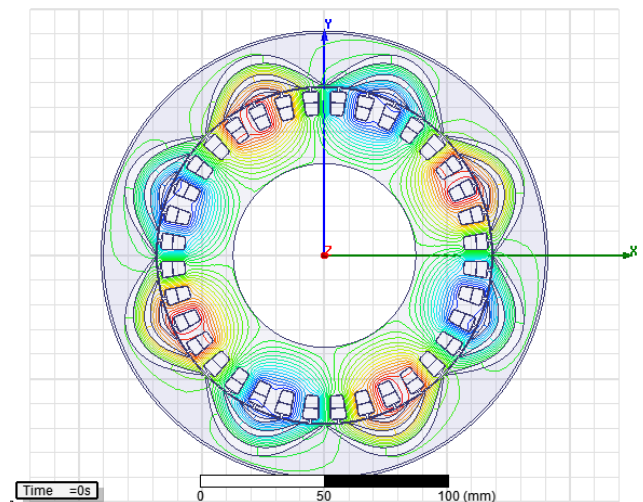

Fig. 2 Flux lines of the 8 pole three flux barriers

All the rotor geometrical parameters are defined with these

World Academy of Science, Engineering and Technology
International Journal of Energy and Power Engineering
Vol:12, No:6, 2018

following assumptions:
- End points of the barrier are distributed uniformly.
- In order to calculate the width of the iron segments, carriers, it is assumed that the average of d-axis MMF along the iron segment is directed into the related iron segment
- Same theoretical design procedure is used to calculate the width of the iron portions in q-axis.

III. Sensitivity Analysis and Simulation Results

In terms of performance improvement, motor inductance plays a key role in the torque development. To study the effect of the shape and dimensions of the flux barriers and carriers on the machine inductances, and consequently on the saliency ratio, several FEA sensitivity analysis with different rotor geometric parameters has been performed. The selected external-rotor synchronous reluctance motor has eight poles, three flux barriers, and 36 stator slots.

A. Air Gap Length

For the SynRM d-axis flux is inversely proportional to the air gap and q-axis flux is inversely proportional to the total air gaps inside the barriers. Because the air gap length is much less than the width of the barriers, the d-axis flux is more sensitive to air gap width changes than the q-axis flux, shown in Fig. 3. Therefore, the difference between two axis fluxes also decreases by increasing the air-gap length. So, considering the mechanical limit, air gap should be kept as thin as possible.
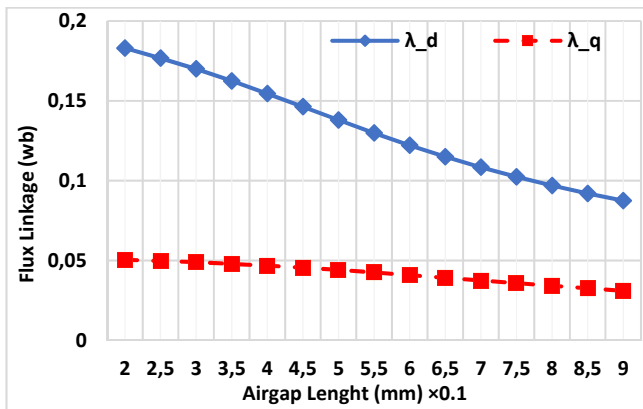

Fig. 3 Effect of air gap length on the d & q-axis fluxes

B. Flux Barriers and Flux Carriers

In this subsection, influence of the barrier width on the saliency ratio, torque, and power factor is studied. The saliency ratio, electromagnetic torque, and power factor for different width of flux barrier and carrier are shown in Fig. 4.
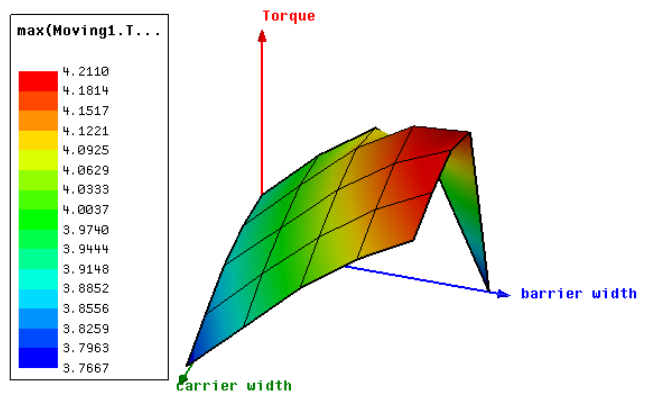
C. Torque vs. Current Angle

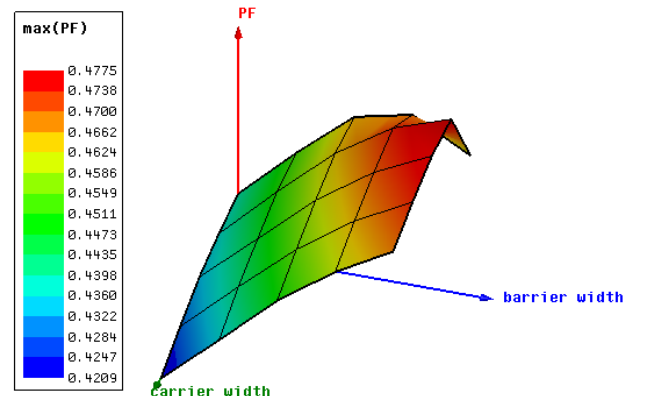Electro-magnetic torque is calculated from:

$$T_{em} = \frac{3}{2}\frac{p}{2}\left(L_{dm} - L_{qm}\right)I_s \sin\left(2\theta\right) \tag{3}$$
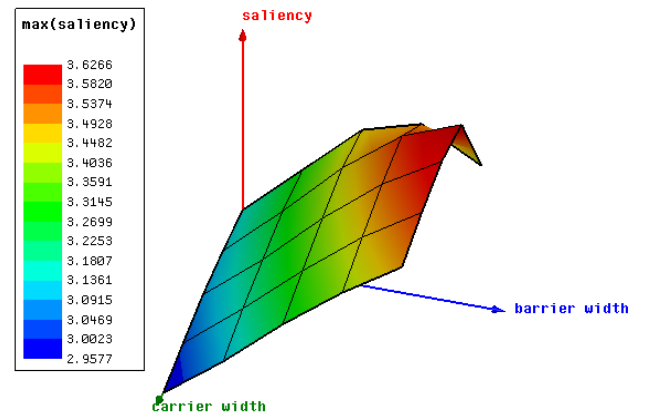
(a)

(b)

(c)

Fig. 4 Surfaces: saliency ratio (a), average torque (b), and power factor (c) for different barrier and carrier width

where I_s is the stator current, θ is the current angle. Equation (3) shows that the torque versus current angle curve has a sinusoidal shape with a maximum at $\theta = 45$deg, but this is not compatible with the FEA results. Two axis fluxes as a function of current angle are shown in Fig. 5. Current angle related to the maximum torque shifts to higher values mainly due to saturation effect. The influence of saturation on the d-axis inductance is reduced by increasing θ beyond 45deg.
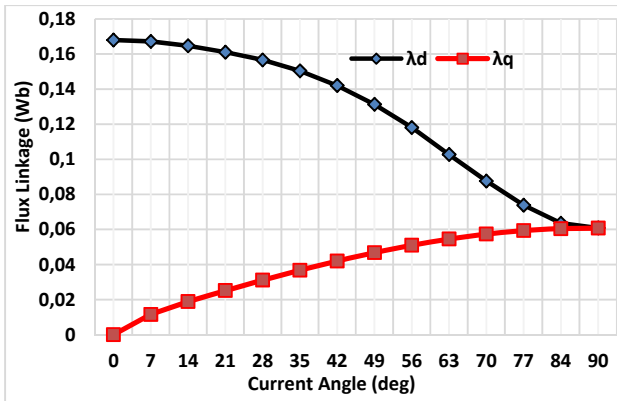
World Academy of Science, Engineering and Technology
International Journal of Energy and Power Engineering
Vol:12, No:6, 2018

Fig. 5 Flux linkage for different current angles

Fig. 6 Flux linkage for different stator current

D. The d-q Axis Inductances for Different Input Currents

The machine inductances are not only a function of stator current but also a function of current angle. In addition, there is cross-coupling between the d-axis and q-axis inductances. Generally, inductance equations can be written as:

$$L_{dm} = L_{qm}\left(i_{dm}, i_{qm}, \theta\right) \tag{4}$$

$$L_{qm} = L_{qm}\left(i_{dm}, i_{qm}, \theta\right) \tag{5}$$

As shown in Fig. 6, the d-axis flux is saturated by an increase in the stator current. The saturation effect in the q-axis inductance is much lower than in the d-axis, because the air insulation barriers cut the q-axis flux. The main responsible of saturation effect in the q-axis would be the presence of the ribs in the rotor topology.

E. Comprasion between SynRM and PMASynRM

There are different reasons, as the following, behind introducing PM into rotor flux barriers: to saturate the rotor iron ribs, to increase the motor torque density, to increase the power factor, as it will be pointed out hereafter. The flux line distribution of the external rotor 8-pole PMaSynRM and its flux density map are illustrated in Fig. 7 and Fig. 8, respectively. When a PM is employed in the rotor flux–barriers, according to (1), it produces a negative flux linkage along the q-axis. So, the q-axis flux linkage versus the current is decreased as reported in Fig. 9. It is shown in Fig. 10 that PMasynRM torque exceeds the developed torque of SynRM as a consequence of adding PM into the third barrier. In order to maintain the fault-tolerant capability of the SynRM, the introduced PM is kept minimum.
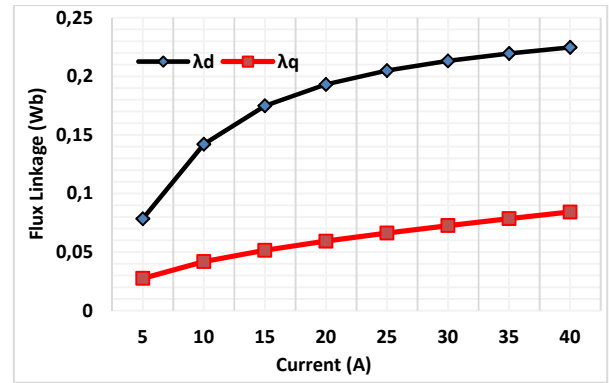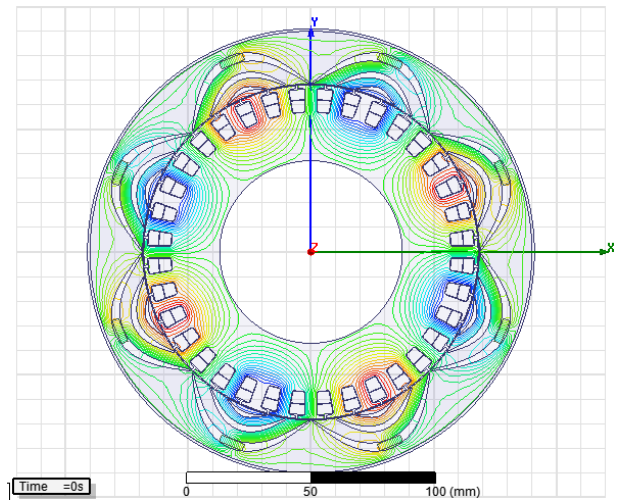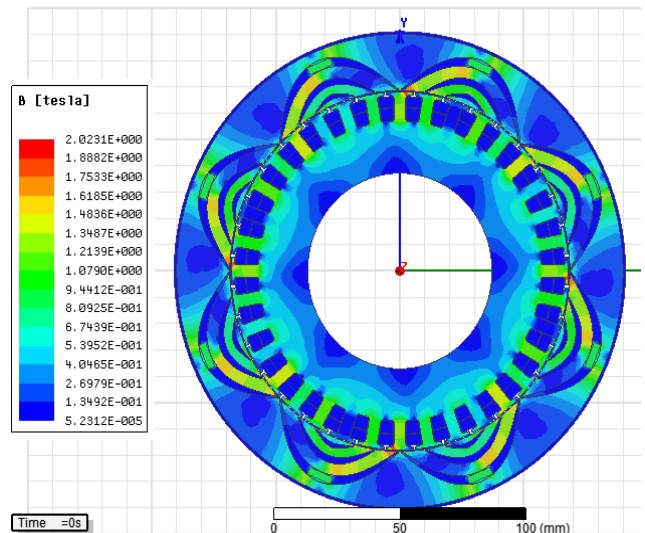

Fig. 7 Flux line distribution of PMaSynRM

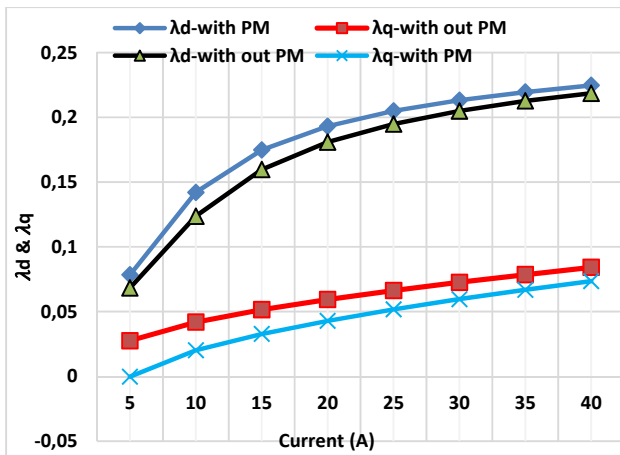Fig. 8 Flux density map for PMaynRM

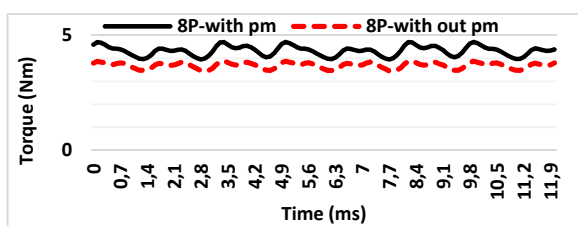Fig. 9 Two axis fluxes for SynRM and PMaSynRM

Fig. 10 Developed torque for SynRM and PMaSynRM

IV. CONCLUSION

This paper deals with external rotor type synchronous reluctance motor and PMaSynRM. A specific set of rotor geometric parameters which have a main influence on the torque density and power factor of the synchronous reluctance motor was considered. According to the simulation results provided by FEA method, width of barrier and carrier in the rotor play a key role in achieving high electromagnetic performance. Also, performance evaluation of PMaSynRM was presented in comparison with SynRM. Consequently, the potential benefit of introducing PM in the rotor flux barrier was revealed. It is concluded embedded PM elevates the torque development capability and power factor of the SynRM.

REFERENCES

[1] J. K. Kostko, "Polyphase reaction synchronous motors," J. Am. Inst. Electr. Eng., vol. 42, no. 11, pp. 1162–1168, 1923.
[2] S. S. R. Bonthu, A. Arafat, and S. Choi, "Comparisons of Rare-Earth and Rare-Earth Free External Rotor Permanent Magnet Assisted Synchronous Reluctance Motors," IEEE Trans. Ind. Electron., vol. 46, no. 330, pp. 1–1, 2017.
[3] L. Jian, K. T. Chau, and J. Z. Jiang, "A Magnetic-Geared Outer-Rotor Permanent-Magnet Brushless Machine for Wind Power Generation," IEEE Trans. Ind. Appl., vol. 45, no. 3, pp. 954–962, 2009.
[4] H. Chen and J. J. Gu, "Switched reluctance motor drive with external rotor for fan in air conditioner," IEEE/ASME Trans. Mechatronics, vol. 18, no. 5, pp. 1448–1458, 2013.
[5] P. J. Holik, D. G. Dorrell, and M. Popescu, "Performance improvement of an external-rotor split-phase induction motor for low-cost drive applications using external rotor can," IEEE Trans. Magn., vol. 43, no. 6, pp. 2549–2551, 2007.
[6] S. S. R. Bonthu, S. Choi, A. Gorgani, and K. Jang, "Design of permanent magnet assisted synchronous reluctance motor with external rotor architecture," in Proceedings - 2015 IEEE International Electric Machines and Drives Conference, IEMDC 2015, 2016, pp. 220–226.
[7] R. A. Inte and F. N. Jurca, "A novel synchronous reluctance motor with outer rotor for an electric bike," in Proceedings of the 2016 International Conference and Exposition on Electrical and Power Engineering, EPE 2016, 2016, no. Epe, pp. 213–218.
[8] Y. Deshpande and H. A. Toliyat, "Design of an outer rotor ferrite assisted synchronous reluctance machine (Fa-SynRM) for electric two wheeler application," in 2014 IEEE Energy Conversion Congress and Exposition, ECCE 2014, 2014, pp. 3147–3154.
[9] S. S. R. Bonthu and S. Choi, "Design procedure for multi-phase external rotor permanent magnet assisted synchronous reluctance machines," in Conference Proceedings - IEEE Applied Power Electronics Conference and Exposition - APEC, 2016, vol. 2016–May, pp. 1131–1137.
[10] M. Z. Islam, S. S. R. Bonthu, and S. Choi, "Obtaining optimized designs of multi-phase PMa-SynRM using lumped parameter model based optimizer," Proc. - 2015 IEEE Int. Electr. Mach. Drives Conf. IEMDC 2015, pp. 1722–1728, 2016.
[11] M. Azhagar Raj and A. Kavitha, "Effect of Rotor Geometry on Peak and Average Torque of External Rotor Synchronous Reluctance Motor (Ex-R SynRM) in comparison with Switched Reluctance Motor for Low Speed Direct Drive Domestic Application," IEEE Trans. Magn., vol. 9464, no. c, pp. 1–1, 2017.
[12] R. R. Moghaddam and F. Gyllensten, "Novel high-performance SynRM design method: An easy approach for a complicated rotor topology," IEEE Trans. Ind. Electron., vol. 61, no. 9, pp. 5058–5065, 2014.
[13] A. Vagati, M. Pastorelli, G. Franceschini, and S. C. Petrache, "Design Of Low-torque-ripple Synchronous Reluctance Motors - Industry Applications, IEEE Transactions on," vol. 34, no. 4, pp. 758–765, 1998.
[14] A. Vagati, "Synchronous Reluctance Electrical Motor having a low torque ripple design", USA patent No. 5,818,140, Oct. 6, 1998.